Host–rabies virus protein–protein interactions as druggable antiviral targets

Usha F. Lingappa[a,1], Xianfu Wu[b,1], Amanda Macieik[a], Shao Feng Yu[a], Andy Atuegbu[a], Michael Corpuz[a], Jean Francis[a], Christine Nichols[a], Alfredo Calayag[a], Hong Shi[a], James A. Ellison[b], Emma K. T. Harrell[a], Vinod Asundi[a], Jaisri R. Lingappa[c], M. Dharma Prasad[d], W. Ian Lipkin[e], Debendranath Dey[a], Clarence R. Hurt[a], Vishwanath R. Lingappa[a,2], William J. Hansen[a,3], and Charles E. Rupprecht[b]

[a]Prosetta Antiviral Inc., San Francisco, CA 94107; [b]Division of High Consequence Pathogens and Pathology, Centers for Disease Control and Prevention, Atlanta, GA 30333; [c]Department of Global Health, University of Washington, Seattle, WA 98102; [d]Prosetta Bioconformatics Pvt. Ltd., Mysore, India; and [e]Center for Infection and Immunity, Mailman School of Public Health of Columbia University, New York, NY 10032

We present an unconventional approach to antiviral drug discovery, which is used to identify potent small molecules against rabies virus. First, we conceptualized viral capsid assembly as occurring via a host-catalyzed biochemical pathway, in contrast to the classical view of capsid formation by self-assembly. This suggested opportunities for antiviral intervention by targeting previously unappreciated catalytic host proteins, which were pursued. Second, we hypothesized these host proteins to be components of heterogeneous, labile, and dynamic multi-subunit assembly machines, not easily isolated by specific target protein-focused methods. This suggested the need to identify active compounds before knowing the precise protein target. A cell-free translation-based small molecule screen was established to recreate the hypothesized interactions involving newly synthesized capsid proteins as host assembly machine substrates. Hits from the screen were validated by efficacy against infectious rabies virus in mammalian cell culture. Used as affinity ligands, advanced analogs were shown to bind a set of proteins that effectively reconstituted drug sensitivity in the cell-free screen and included a small but discrete subfraction of cellular ATP-binding cassette family E1 (ABCE1), a host protein previously found essential for HIV capsid formation. Taken together, these studies advance an alternate view of capsid formation (as a host-catalyzed biochemical pathway), a different paradigm for drug discovery (whole pathway screening without knowledge of the target), and suggest the existence of labile assembly machines that can be rendered accessible as next-generation drug targets by the means described.

assembly intermediate | viral–host interaction | whole pathway screen | drug discovery paradigm | protein heterogeneity

Rabies virus (RABV) poses a worthwhile challenge for antiviral drug discovery (1). Despite the existence of an effective vaccine, more than 50,000 humans die of rabies annually worldwide (2). [In fact, this estimate is likely very low, because many human rabies cases occur in areas where incidence is underreported by up to 100-fold (2).] Because vaccine efficacy for postexposure prophylaxis is strictly time limited, millions more are at risk, even in areas with adequate health care resources (3). Upon onset of symptoms, the disease has a nearly 100% case fatality rate (4), making it arguably the most deadly viral disease of humans, and no effective small-molecule therapeutic has been found previously. A drug that is inexpensive to produce, that can be stored at room temperature, thereby facilitating distribution and access, and that demonstrates efficacy during the symptomatic stage of the disease would address this ancient and significant public health need.

The lifecycles of all viruses involve variations on a common theme. A viral particle must release its genome inside a host cell, replicate its genetic information, express encoded proteins, and assemble capsids (the protein shell that protects the viral genome) before completing formation/maturation and release of new viral particles. Capsid assembly is a highly efficient process,

often occurring in organized structures that have been described as "viral factories" (5). Although catalytic roles for host proteins are recognized for most steps in the viral lifecycle, capsid assembly still is viewed commonly as a spontaneous, thermodynamically driven process termed "self-assembly" (e.g., refs. 6 and 7).

However, studies in three diverse viral families, HIV (8–13), hepatitis B virus (14), and hepatitis C virus (15, 16), suggest a very different path to capsid formation. In this alternative view, capsid assembly occurs via discrete assembly intermediates within a biochemical pathway involving energy-dependent and host factor-dependent steps. Based on these studies, we hypothesized that analogous events occurred in RABV capsid assembly and that viewing capsid assembly as a concerted biochemical process including critical host protein-catalyzed steps would prove productive when applied to drug discovery. Likely participants in such steps would be protein machines involved in other assembly events for the host that are commandeered upon viral infection, manipulated, and possibly modified to meet the needs of the virus for capsid assembly. Host assembly machines that have been optimized for the virus rather than for the host (e.g., by viral manipulation of host-signaling pathways) are promising antiviral targets that likely can be blocked without substantial toxicity; although they are composed of host proteins, their loss should not impair a host function, only propagation of the virus. Perhaps previous efforts to develop anti-capsid therapeutics have been disappointing precisely because they did not target the hypothesized host enzymes of capsid formation but rather attempted to block capsid protein interactions directly (17, 18).

The identification of druggable targets remains a substantial hurdle facing contemporary small-molecule drug discovery (19). [The term "druggable targets" is defined by Hopkins et al. (19) as targets that are able to bind compounds with the properties of a commercially viable drug (i.e., compounds that are orally bioavailable and conform to Lipinski's rule of five) (20).] Conventional targets soon will be exhausted, and the likely highly unconventional targets of the future remain elusive to prevailing approaches (20). We believe that many highly druggable targets, including the assembly machines hypothesized here, have been
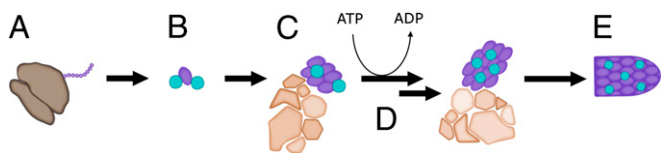
Fig. 1. Cartoon of the proposed RABV capsid-assembly pathway, based on our findings and data in the literature cited. (*A*) Nascent RABV N. (*B*) P associates with unassembled N monomers (30–34). (*C*) One or more host multiprotein complex is hypothesized to facilitate capsid assembly. (*D*) The capsid-assembly pathway involves energy-dependent steps. (*E*) Completed capsid. Interference with this pathway by energy depletion, host factor depletion, or small-molecule activity can block progression along the pathway or lead to off-pathway interactions and the formation of aberrant capsids.

missed because conventional drug discovery typically starts with target identification. However, if the target is a labile multiprotein complex (MPC) that defies conventional purification, and if such MPCs are highly heterogeneous with small, discrete, and nonoverlapping subsets of the component proteins serving as parts of different assembly machines, then unorthodox approaches would be necessary to pursue such targets.

During the last decade, there has been a growing appreciation of the abundance and diversity of MPCs within the cell (21–23). MPCs represent the core of the protein–protein interaction (PPI) networks responsible for a multitude of biological functions (23, 24). Effective therapeutic modulation of MPC PPIs would be powerful (25, 26), but a history of unsuccessful attempts has led to the widespread opinion that such targets are not druggable (19). We hypothesize that these setbacks can be attributed to the limitations imposed by both traditional drugs and traditional approaches to drug discovery and that a different approach might be successful. First, most existing small-molecule drugs achieve their activity by competing directly with an endogenous molecule for a functional binding site (19). This type of mechanism is not easily applied to MPCs, which often involve large binding surfaces, weak affinities, transient interactions, and disordered protein regions (26, 27). Biological systems generally modulate PPIs through allostery rather than direct inhibition, indicating that binding an allosteric site is much more likely to be an effective mechanism for drug action against MPC targets (26). Second, the predominant approach to drug discovery involves identifying a specific target before finding a lead compound, thereby limiting discovery to targets of sufficient stability for conventional purification. Labile complexes of loosely associated proteins that are unstable (at least once the cell is disrupted) therefore are not readily amenable to standard purification techniques. Thus, perhaps the biggest obstacle to identifying drugs that

target MPCs is that the MPCs themselves can be missed by target-based drug-discovery programs.

As an alternative to a target-based program, we propose functional reconstitution of critical PPIs involved in the capsid-assembly pathway following de novo synthesis of the capsid protein as a putative assembly substrate. If even a portion of the capsid-assembly pathway involving newly synthesized capsid proteins has been reconstituted, it can be converted readily into a screen for the identification of small molecules that block any earlier step in the pathway—without knowledge of the target. Hits from this screen can be validated by their activity against infectious virus in cell culture and then subjected to optimization of the structure–activity relationship (SAR) to establish quickly whether their targets are truly druggable. The successfully advanced compounds themselves then can be used as affinity ligands to fractionate the starting extract (before translation of the viral capsid protein mRNA) far more rapidly than could be done without the drug-based affinity ligand. The protein(s) bound to the affinity ligand that are eluted specifically by free compound would comprise the drug target. The identity of the target can be confirmed by comparing assembly reaction products from starting, fractionated, target-depleted, and target-reconstituted extracts. Thus, a classical cell biological approach, de novo cell-free protein synthesis (CFPS) (28), is used effectively to turn conventional drug discovery on its head: to find the compound first by using a whole pathway screen and to identify the target later by advanced analog affinity chromatography, validated by functional reconstitution of the hypothesized assembly pathway. Here we successfully demonstrate this approach for RABV and show that the drug target has the hypothesized unconventional properties.

Results and Discussion

RABV Assembly Pathway. RABV has a nonsegmented negative-strand RNA genome that codes for five proteins: the nucleoprotein (N), the phosphoprotein (P), the matrix protein (M), the glycoprotein (G), and the large protein (L). Together, L and P comprise the viral polymerase. N encapsidates the RNA genome in a tight helical RNase-resistant ribonucleoprotein (RNP) capsid (29). P has been shown to associate with N (30, 31) before RNP capsid assembly at a P:N ratio of 2:1, in contrast to the 1:2 ratio found in the completed capsid (32–34). Formation of the RNP capsid is followed by virion assembly and budding, models for which can be found in the literature (29). These models emphasize the multiple roles of M, which include condensing the RNP complex and coordinating budding by associating with both the capsid and budding sites on the cell membrane designated by microdomains of transmembrane G. Because of the complexity
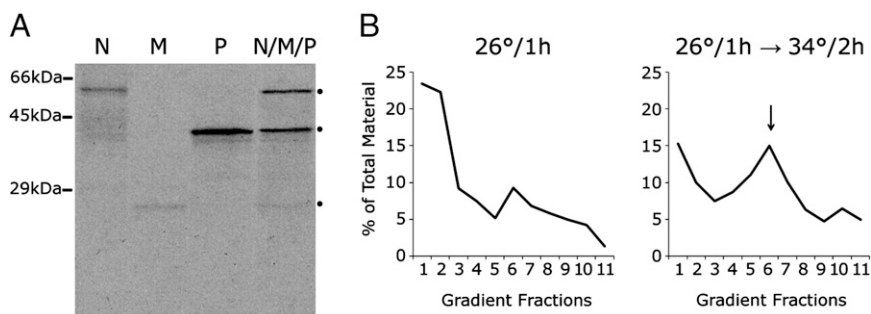

Fig. 2. (*A*) Autoradiogram of ^{35}S-radiolabeled CFPS translation products of the N, M, and P genes of RABV, individually and when coexpressed, as analyzed by SDS/PAGE. Major bands correspond to the expected sizes of the RABV N, M, and P proteins. (*B*) Sucrose gradient quantification of RABV N expression in a CFPS reaction programmed with RABV N, M, and P mRNA under synthesis (26 °C for 1 h) (*Left*) and subsequent assembly conditions (26 °C for 1 h → 34 °C for 2 h) (*Right*). Note the progression of N from being predominantly at the top of the gradient after synthesis, diminishing in material at the top of the gradient, and increasing in the peak in fraction 6 after incubation (*Right*, downward pointing arrow).
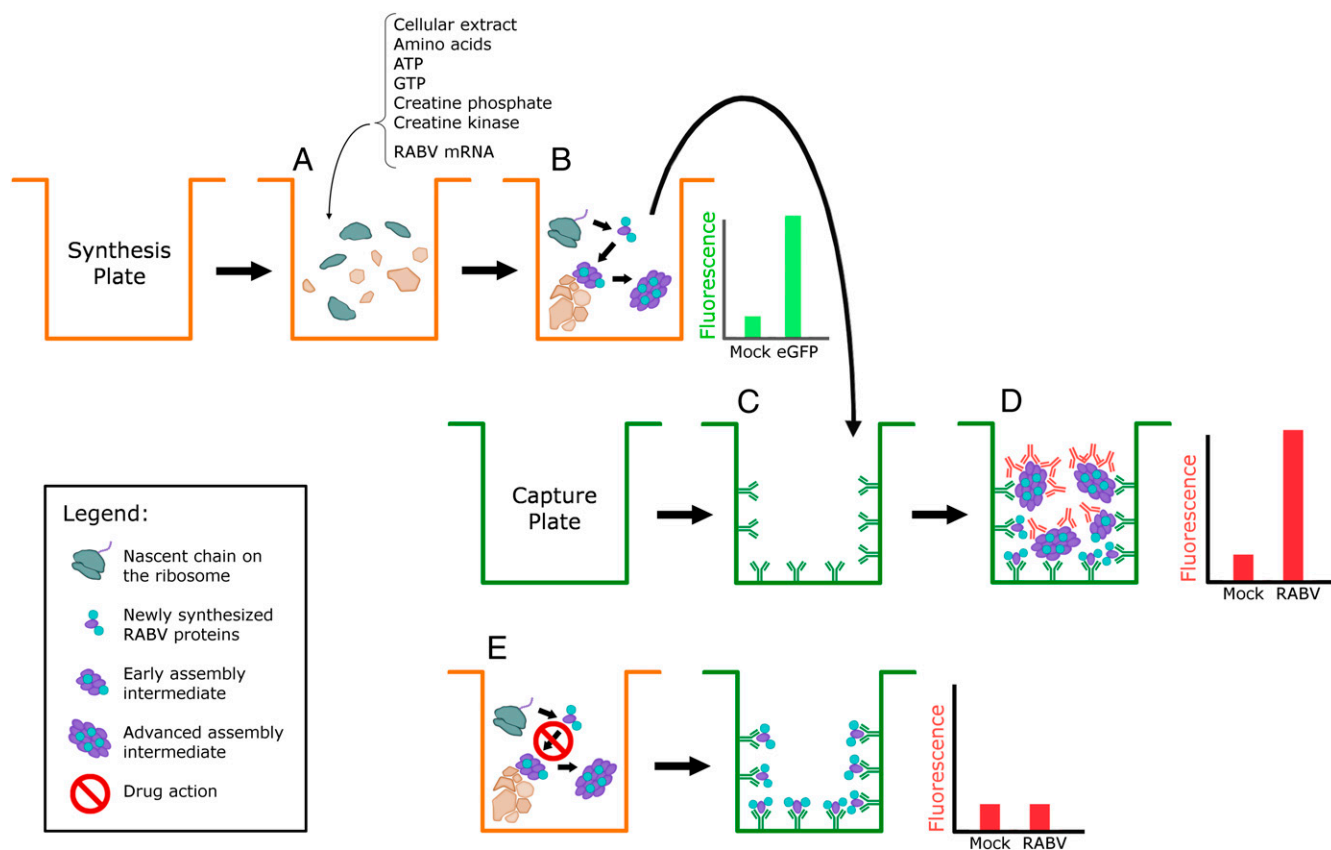
Fig. 3. Diagram of the CFPS whole-pathway plate screen. (*A*) CFPS system consisting of cellular extract, RABV N, M, and P mRNAs, eGFP mRNA, amino acids, and an energy-regenerating system. (*B*) Hypothesized synthesis and assembly of RABV capsid proteins occurring during the sequential incubation steps described in Fig. 2. (*C*) CFPS translation products transferred to a capture plate previously coated with anti-RABV N affinity-purified antibody. (*D*) RABV N bound to the capture plate is decorated with biotinylated secondary antibody, which is used to generate a fluorescent readout. (*E*) Drug treatment that blocks the formation of large N multimers or that results in the formation of aberrant structures that mask epitopes results in inhibition of fluorescence. To ensure diminution in fluorescence is not caused by inhibition of protein synthesis, eGFP is cotranslated with RABV proteins, and the extent of eGFP fluorescence is monitored before transfer to the capture plate. Compounds whose inhibition of N-derived fluorescence is comparable to the inhibition of eGFP fluorescence are likely to be false positives.

of M and P interactions with N, all three viral genes were coexpressed by CFPS. For the purposes of the present study, we simply need (*i*) to hypothesize that such interactions occur (Fig. 1); (*ii*) to show that those interactions are broadly resolvable into two steps, one predominantly for synthesis of the RABV proteins and another to enhance assembly into large structures (Fig. 2); (*iii*) to convert those reactions into a whole-pathway screen; and (*iv*) to make testable predictions regarding validation
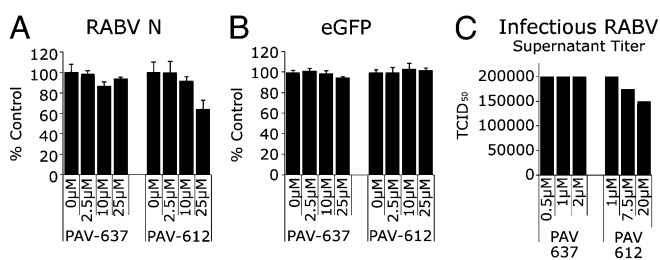

Fig. 4. (*A*) Detection of active compound PAV-612 compared with inactive compound PAV-637 by CFPS plate screen. Assembly is measured in relative fluorescent units (RFU). Error bars represent SD of triplicates. (*B*) Fluorescence of cotranslated eGFP, demonstrating that the observed drug effect is not inhibition of protein synthesis. (*C*) PAV-612 activity corroborated by 50% tissue culture infective dose ($TCID_{50}$) assessment in Vero cells 40 h after infection.

of hits from that screen against infectious RABV in cell culture (see below).

RABV CFPS Drug Screen. To use CFPS programmed with RABV gene products for the identification of small molecules that block or alter progression through the hypothesized assembly pathway, we first demonstrated that synthesis of RABV N, P, and M proteins, individually or together, in a wheat germ (WG) CFPS at 26 °C for 1 h results in protein products of the correct size (Fig. 2*A*). When the translation products were analyzed by sucrose step gradients, they localized predominantly to the top of the gradients (Fig. 2*B*, *Left*). Upon subsequent incubation at 34 °C for 2 h, followed by the same gradient analysis, RABV N was converted to higher molecular weight complexes (Fig. 2*B*, *Right*). By analogy to previous studies of capsid protein expression by CFPS (12, 14, 35–37), we hypothesized that the high molecular weight RABV complexes containing N represented the culmination of myriad PPIs in a RABV capsid-assembly pathway.

We then devised a fluorescent plate assay to monitor the formation of multimeric N-containing structures (Fig. 3). RABV N, M, P, and eGFP mRNAs were translated by CFPS in 384-well format in the absence or presence of small molecules under the conditions shown in Fig. 2*B* to achieve both synthesis and putative RABV assembly. Coexpression of eGFP, an unrelated protein that is inert in the capsid-assembly process, serves to measure effects of individual small molecules on protein syn-
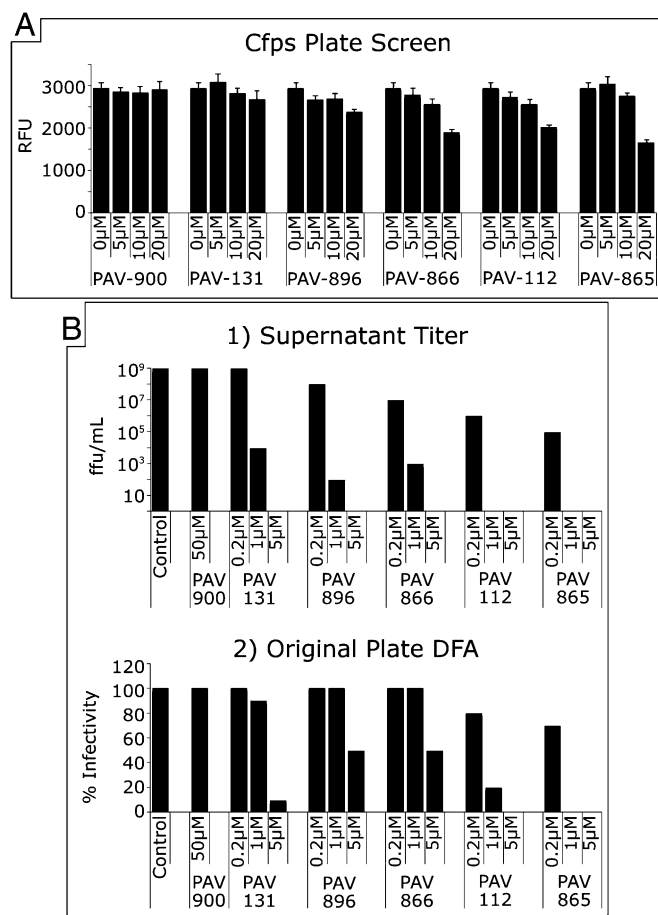
Fig. 5. (A) Analogs to PAV-612 demonstrating a robust SAR on the CFPS plate screen. Error bars represent SD of triplicates. (B) Activity of PAV-612 analogs against infectious RABV in Vero cells as assessed by measurement of focus-forming units per milliliter of the medium (*Upper*) and by DFA assay of the cells in the primary infection plate (*Lower*).

thesis. Diminution of eGFP fluorescence allows us to distinguish hits that merely inhibit protein synthesis from those that block capsid assembly. Products then were captured on a second 384-well plate coated with affinity-purified antibody to RABV N (anti-N), and decorated with biotinylated anti-N. The bound biotinylated antibody was used to generate a fluorescent readout. When a monomer of N is captured, its single epitope is occupied, and there are no exposed epitopes to bind biotinylated antibody. However, either completed capsids or even assembly inter-mediates, comprising many copies of N, should expose epitopes in excess of that used for capture and should give a robust fluorescent signal. If a small molecule present in the synthesis plate disrupts any step in the assembly process, epitope exposure is likely to change, and therefore the fluorescent signal should change, in a dose-dependent fashion. A portion of the Prosetta compound collection, comprising small molecules conforming to Lipinski's rule of five (38), was screened, and compounds showing selective dose-dependent change of N fluorescence were iden-tified as hits.

Compound Advancement. We identified a small set of modestly active compounds in the CFPS screen and assessed these in Vero cells against a strain of "street rabies" isolated from a rabid gray fox. Fig. 4 shows the data from an active compound, PAV-612, compared with an inactive compound, PAV-637. A set of ana-logs then was synthesized and assessed in both the CFPS screen

(Fig. 5A) and against infectious RABV in cell culture (Fig. 5B). These analogs demonstrate a robust SAR for efficacy, suggesting an excellent starting point for anti-RABV drug discovery. The extent of activity on the screen corresponds roughly to the degree of activity observed against infectious RABV in cell culture. These results validate our CFPS-based screen, support our working hypotheses on capsid assembly, and highlight the value of a whole-pathway screen as outlined above.

One analog, PAV-866 (Fig. 6A), was chosen for further study. PAV-866 has an EC_{50} against infectious RABV in Vero cell culture of ~15–30 nM (Fig. 6B) and eliminates all RABV in-fectivity (>9 logs) in the low μM range. When assessed for toxicity in Vero cells, this compound was found to have a 50% cytotoxic concentration (CC_{50}) of ~2.5–10 μM. Thus, the selectivity index (SI) or CC_{50}/EC_{50} of this compound was ~100. Although other compounds in this chemical series (such as PAV-112 and PAV-865) were more potent than PAV-866 against infectious RABV in cells, they also were more toxic and therefore had a lower SI.

Time of Drug Action. If these compounds act on host factors that play a catalytic role in viral capsid assembly, their efficacy should depend on the addition of the compound within the hypothe-sized time frame of action, i.e., during capsid protein synthesis and assembly. In cell culture we compared the effect of various times of PAV-866 addition (1–12 h after infection) on the in-fectivity of the medium harvested 72 h after infection. If, con-trary to our hypothesis, the compounds acted directly on the progeny virus, infectivity would be eliminated equally regardless of the time at which the compound was added during the first 12 h of the 72-h time course, because the compound would still have the opportunity to act on the virus in the medium before
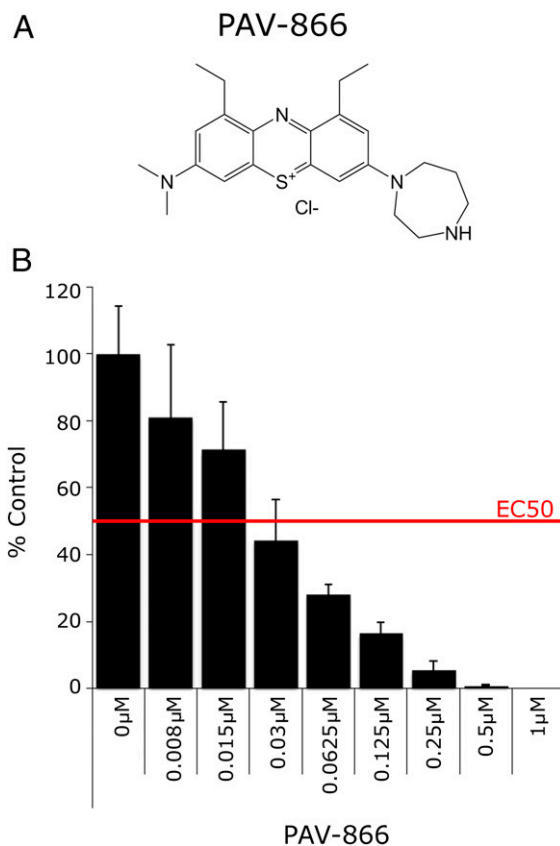

Fig. 6. (A) Structure PAV-866, a small molecule (FW = 432). (B) PAV-866 has potent activity against RABV in cell culture in the low nanomolar range.
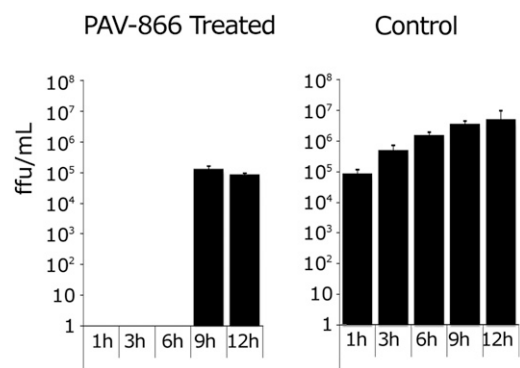
Fig. 7. Effect of time of addition on PAV-866 action against RABV in cell culture. Drug was added at various times ranging from 1 to 12 h after infection, and efficacy was assessed by determining the number of focus-forming units per milliliter of medium 72 h after infection.

harvest. As shown in Fig. 7, the efficacy of PAV-866 diminishes strikingly when it is added at times beyond 6 h postinfection. This result is consistent with compound action on intracellular targets within the proposed host-catalyzed capsid-assembly pathway.

Target Isolation, Depletion, and Reconstitution. If, as proposed, these compounds target a labile assembly machine that is an MPC, it may be possible to take advantage of the high affinity of PAV-866 for the functional target to isolate the hypothesized MPC by affinity chromatography, a protein-separation method that exploits the specific interaction between an immobilized ligand and proteins of interest (39). PAV-866 was coupled to a resin (termed column 124) and used as an affinity ligand for column chromatography. A column of blocked resin without compound (column 74) served as a negative control for binding specificity. The starting WG extract (before its use for CFPS expression of RABV proteins) was applied to the columns. Columns were washed with 50 bed volumes of buffer and then were incubated with free PAV-866 to elute proteins bound specifically to the ligand. SDS/PAGE and silver-stain analysis of the eluate revealed a striking set of proteins that bound specifically to column 124 and not to column 74 and that were eluted with free compound (Fig. 8A). Affinity chromatography of mammalian brain postmitochondrial supernatant (PMiS) produced a pattern of proteins similar to that seen in the eluate from WG extract that is used for CFPS (Fig. 8B). Concurrence of the set of binding proteins from both plant and brain extracts suggests a conserved set of PPIs and is remarkable, given RABV neurotropism. RABV capsids generated by Triton X-100 treatment of irradiated authentic RABV showed no specific binding to column 124, reinforcing our earlier conclusion that the drug target is a host cellular protein rather than a viral protein (Fig. 9).

To verify that the factors that bound column 124 indeed included the drug target, we collected the WG extract column flow-through depleted of PAV-866–resin conjugate-bound proteins. CFPS reactions carried out in depleted extract lack the dose-dependent drug effects seen in the plate screen using the starting extract (Fig. 10 A and B), indicating that the target was missing from the 124 column flow-through. However, when the depleted extract is reconstituted with column 124 eluate (exhaustively dialyzed to remove both free and bound drug), the dose-dependent drug effect is restored fully (Fig. 10C), confirming that the eluate contains the drug target.

Drug Target Composition. ATP-binding cassette family E1 (ABCE1), a host protein formerly known as "HP68" (40) and "RNase L inhibitor" (41), has been implicated in various activities including ribosome recycling (42–46) and HIV capsid assembly (8–11, 13, 40).

By Western blotting with an affinity-purified antibody raised to a C-terminal epitope of ABCE1, we show the presence of ABCE1 in both WG and PMiS column 124 eluates (Fig. 8C).

Starting extracts that were analyzed by glycerol gradient ultracentrifugation and then Western blotted for ABCE1 displayed an extremely heterogeneous distribution across the gradient (shown for PMiS in Fig. 11, *Top*) When individual gradient fractions were applied to drug columns, only a very small portion of total ABCE1, belonging to a single discrete subfraction migrating predominantly in glycerol gradient fraction 3 and accounting for ~1–5% of total cellular ABCE1, is bound to the column (Fig. 11, *Middle*). This result suggests that only a small subset of the total ABCE1 present in the cell is incorporated into the MPC relevant for the step in RABV capsid formation targeted by PAV-866. These data are consistent with the hypothesized heterogeneity and unconventional properties of the MPC comprising the drug target.

It is remarkable that only a tiny subfraction of total host ABCE1 was found to be competent to bind the PAV-866 resin conjugate. Because each gradient fraction was assessed independently for drug binding, the failure of the great majority of ABCE1 to bind suggests substantial heterogeneity of ABCE1, rendering conventional proteomic and molecular biological methods (e.g., siRNA knockdown) unlikely to be able to distinguish the minor subfraction likely to represent the true PAV-866 target. Hence, without the unconventional approach and unorthodox hypotheses presented here, the target MPCs and the drugs that block them likely would not have been identified.

Conclusions

Previous studies used CFPS to achieve faithful assembly of capsids for multiple families of viruses (12, 14, 16). We therefore approached antiviral drug discovery from the perspective of the capsid protein being the substrate for a host-catalyzed biochemical pathway driven by an MPC. We further hypothesized the reasons for the failure of previous studies either to develop effective anti-capsid compounds or to detect roles for catalytic host-derived capsid-assembly machines and established an approach by which these obstacles might be circumvented and the
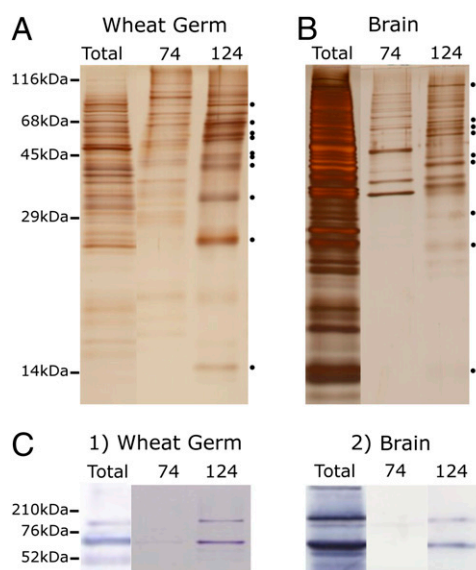

Fig. 8. Silver-stained SDS/PAGE showing the banding pattern of total extract, PAV-866 eluates from column 74, and PAV-866 eluates from column 124 for (A) WG extract and (B) PMiS. (C) Western blot of the 68-kDa ABCE1 protein from WG extract column 124 PAV-866 eluates (*Left*) and PMiS column 124 PAV-866 eluates (*Right*).
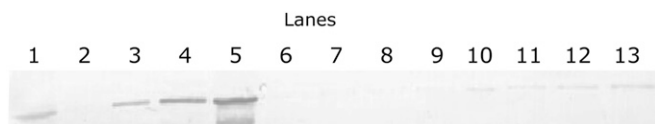
Fig. 9. Western blot of authentic RABV capsids' binding affinity to columns of resins 124 (PAV-866 conjugate) and 74 (negative control). Lane 1 shows an aliquot of flow-through that did not bind to column 124. Lanes 2–5 show a serial dilution of authentic capsid starting material, demonstrating the limits of detectability by Western blot (~0.1% of input). Lanes 6–9 and 10–13 are first, second, and overnight eluates and a urea wash from columns 124 and 74, respectively. No specific binding to 124 resin columns (lanes 6–9) compared with control 74 resin columns (lanes 10–13) is detectable.

hypothesized MPC-assembly machines identified. We used RABV as a test case. A cell-free de novo synthesis screen was established and used to identify hits whose efficacy was validated against infectious RABV in mammalian cell culture. The active compounds were subjected to SAR optimization, and an advanced analog coupled to resin was used for affinity chromatography to identify the targets. A set of proteins, including ABCE1, a host protein previously shown to be essential for HIV capsid formation, was identified by free drug elution from the drug resins and was shown to include the drug target collectively by functional reconstitution of drug sensitivity in the same CFPS screen by which the active compound was identified in the first place. It should be noted that these studies have not established whether ABCE1 is the direct (nearest neighbor) PAV-866–binding protein. It also is possible that ABCE1 is involved in multiple steps or that different subsets of ABCE1 play different roles in the capsid-assembly process. Further studies with the system, tools, and reagents described here should clarify these issues.

The work presented here was predicated on the hypothesis of host catalysis (47) of capsid formation by labile MPCs and was designed to overcome pitfalls of conventional antiviral drug discovery. When applied to RABV, a virus for which no antiviral therapy currently exists, this approach successfully identified compounds of striking antiviral potency and excellent therapeutic index in cell culture, whose target appears to be a labile host MPC comprising highly heterogeneous protein components. If host protein functional heterogeneity in assembly machines is as massive as implied by this study, and if, as suggested, such MPCs are viable drug targets, the approach taken here to identify antiviral compounds may have broader applications to next-generation drug discovery not limited to antiviral therapeutics.

Materials and Methods

Materials were purchased from Sigma Chemical Co. or Thermo Fisher, unless otherwise noted. Affinity-purified antibodies to RABV N and ABCE1 are available from www.prosetta.co.in.

Cell-Free Transcription and Translation. Coding regions of interest (RABV N, P, and M) were engineered behind the SP6 bacteriophage promoter and the *Xenopus* globin 5′ UTR. DNA was amplified by PCR and then transcribed in vitro to generate mRNA encoding each full-length protein. Translations were carried out in the WG CFPS system either supplemented with ^{35}S amino acid or with all 20 nonradiolabeled amino acids, as previously described (12, 14) but at reduced concentrations of WG extract. Samples in Fig. 2 were radiolabeled, allowing their direct detection by SDS/PAGE and autoradiograph; those used for the CFPS plate screen (Figs. 4 and 5) were not radiolabeled and were detected by antibody capture and detection as described in Fig. 3.

Sucrose Step Gradients. Sucrose step gradients were performed as previously described (12, 14) and were analyzed by SDS/PAGE, autoradiography, and quantification of RABV N band density.

Moderate-Throughput Small-Molecule Screening. Moderate-throughput small-molecule screening was carried out in a 384-well format by translation of eGFP and RABV N, P, and M mRNA in the presence of small molecules from the

Prosetta compound collection. Reactions were run at 26 °C for 1 h for synthesis, followed by assembly at 34 °C for 2 h. eGFP fluorescent readout was measured at 488/515 nm (excitation/emission). Products were captured on a second 384-well plate precoated with affinity-purified antibody. Plates were washed with PBS containing 1% Triton X-100, decorated with biotinylated affinity-purified antibody, washed, detected by NeutrAvidin HRP, washed again, and then incubated with a fluorogenic HRP substrate Quanta Blue for 1 h. Fluorescent readout was measured at 330/425 nm (excitation/emission). Relevant reagents were obtained from Pierce Protein Research Products.

Antibody Generation. A peptide epitope of RABV N exposed on the surface of RABV capsids (48), CFFRDEKELQEYEAAELTKTVDALADD, with N-terminal acetylation and C-terminal amidation to mimic its internal position in the RABV N sequence, was chosen for coupling to carrier and immunization of rabbits, and polyclonal rabbit antibodies were generated as described (49). Bleeds were screened by Western blot and immunoprecipitation of radiolabeled RABV N products. High-titer sera were pooled and affinity purified as described.

Cells and Virus. Street RABV (TxFX A11-1198), associated with enzootics in carnivores throughout the southwest United States, was derived from the salivary glands of a rabid gray fox (*Urocyon cinereoargenteus*). Mouse neuroblastoma (MNA) cells were propagated in Eagle minimal essential medium supplemented with 10% FBS. In multiple wells of a 96-well plate, MNA cells (except control cells) were infected with RABV at a multiplicity of infection (MOI) of 0.1 per cell and were incubated at 37 °C for 48 h in the presence of MEM supplemented with 10% FCS. Then 100 μL of supernatant was removed from each well and replaced with an antiviral compound at described concentrations. Cells were incubated for an additional 48 h.

RABV Infectivity Titration. After incubation, 100 μL of supernatant was removed and titrated on MNA. Microtiter plates were washed twice in PBS
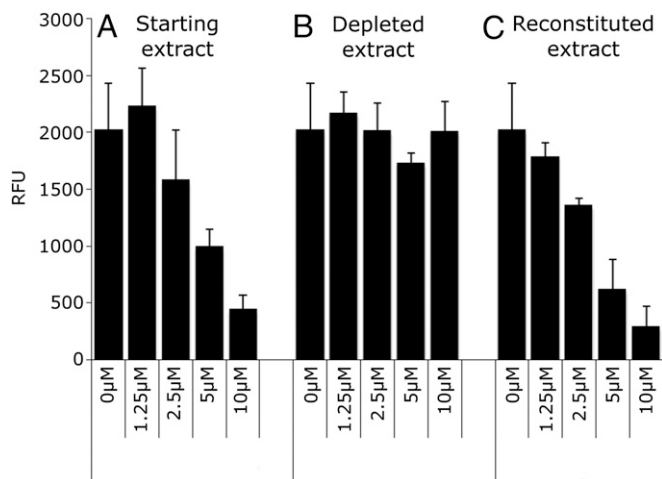

Fig. 10. Plate assay profiles of CFPS reactions in the presence of a titration of a PAV-866 analog carried out in (*A*) starting, (*B*) depleted, and (*C*) reconstituted cellular extracts. Reactions carried out in starting extracts show familiar dose–response curves, reactions carried out in depleted extracts show no drug effects, and reactions carried out in reconstituted extracts show a full restoration of dose-dependent drug effect. Error bars represent SD of triplicates. The presence of full RFUs but no drug effect in the absence of target (upon expression in the depleted extract, *B*) and restoration of drug effect upon target protein reconstitution by the addition of dialyzed free drug eluate (upon expression in reconstituted extract, *C*) is consistent with the hypothesis that the plate screen is not a simple readout of multi-merization. Loss of RFUs upon drug treatment in the presence of target is likely due to formation of aberrant structures in which the relevant epitopes are masked. It is not surprising that the consequence of target depletion itself is different from the consequence of treatment with the drug used as an affinity ligand to achieve target depletion. In the former instance, one of the capsid-assembly factors is missing; in the latter instance, the assembly factor is present but nonfunctional (because of drug action), perhaps conferring the equivalent of a dominant negative phenotype.
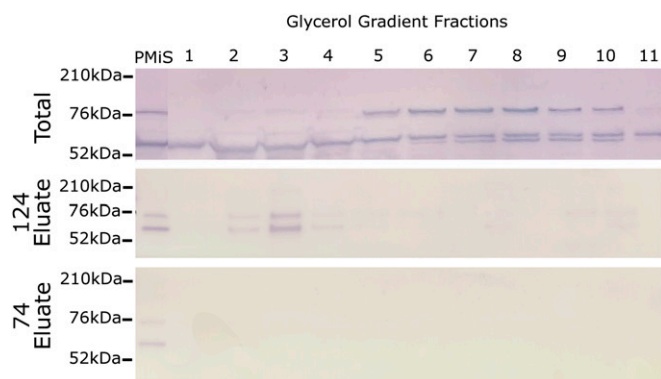
Glycerol Gradient Fractions

Fig. 11. Starting PMiS glycerol gradient fractions and their column eluates analyzed by Western blot with anti-ABCE1. Note the heterogeneity of ABCE1 not only in the size of the immunoreactive protein species (presumably because of posttranslational modifications) but also across the gradient as demonstrated by drug column binding being limited largely to fraction 3. Note also that the ~70-kDa isoform that is a minor species in the total gradient fraction 3 (*Top*) is greatly enriched in the column 124 free drug eluate (*Middle*). The *Bottom* panel is the eluate of each glycerol gradient fraction applied to the control column 74 (blocked resin), demonstrating the specificity of the ABCE1 immunoreactivity seen in fraction 3 of the *Middle* panel.

(pH 7.2–7.4) and fixed with 80% acetone at −20 °C. RABV antigens were detected by direct fluorescent antibody staining using FITC-labeled monoclonal antibody conjugate (Fujirebio Diagnostics, Inc.). Titers for infectious virus released into the supernatant were calculated by the Reed and Muench method. The BSR cells [a clone of baby hamster kidney (BHK) cells] were grown in DMEM supplemented with 10% FBS (Atlanta Biologicals) at 37 °C in a 5% CO_2 incubator. The RABV ERA strain was obtained from The American Type Culture Collection and maintained at The Centers for Disease Control and Prevention in Atlanta. For virus titration and antiviral compound treatment, the confluent BSR cells in T75 flasks were split and seeded to a 24-well plate (Fisher Scientific). After 24 h incubation, the confluent BSR cells in the plate were infected with 1 MOI of RABV ERA either before or after treatment with the antiviral compound at the indicated time course. The virus titer in the treated cell supernatants was calculated in focus-forming units (ffu) per milliliter. In brief, 20 µL of cell supernatants mixed with 180 µL of freshly prepared BSR cell suspension was seeded into a Lab-Tek Chamber Slide (Fisher Scientific). A serial 10-fold dilution of the virus–cell supernatants was made with similar BSR cell suspensions in the same slide. The cells were incubated at 37 °C in a 5% CO_2 incubator for 24 h before titration using the direct fluorescent antigen (DFA) assay. A standard DFA protocol (www.cdc.gov/rabies/pdf/rabiesdfaspv2.pdf) was followed for virus

titration for the effect of antiviral compound treatment against the original cells grown in the 24-well plate.

Affinity Chromatography. Compound resin conjugate (50–100 µL) was equilibrated in a buffer containing 50 mM Hepes or triethanolamine (pH 7.5), 0.35% Triton X-100, and 0.2 mM thioglycolate (pH 7.5). Up to 50 uL of sucrose step gradient fraction was applied. The column was clamped and incubated at 4 °C for 1 h and then washed with 100 bed volumes of the same buffer. One bed volume of free compound at 200 µg/mL (approaching its maximum solubility in water) was added, the column was clamped for 1 h, and three serial eluates were collected. The column then was washed extensively, clamped for 1 h in 8 M urea, washed further, and equilibrated in isopropanol for storage. Column eluates were subjected to exhaustive dialysis to remove both free and bound compound.

Authentic Irradiated RABV. Authentic irradiated RABV was treated with Triton X-100 to solubilize the envelope and release the capsid and then was applied to columns of resins 124 (PAV-866 conjugate) and 74 (negative control). Later, columns were incubated with free compound to elute bound proteins and were washed with urea. Western blots of authentic capsids were probed with anti-N.

Glycerol Gradients. Glycerol gradients were poured using a linear gradient former from 5–35% glycerol in 10 mM triethanolamine (pH 7.6), 10 mM NaCl, 1 mM magnesium acetate, and 0.2 mM EDTA. Samples up to 200 µL were loaded onto chilled gradients and centrifuged in a TL-100 Beckman centrifuge using a TLS-55 swinging bucket rotor at 50,000 rpm for 55 min with slow acceleration and deceleration. Gradients were fractionated into eleven 200-µL aliquots and analyzed by SDS/PAGE.

SDS/PAGE. SDS/PAGE was carried out as previously described (12, 14).

Western Blotting. For Western blotting, SDS/PAGE gels were transferred in Towbin buffer to polyvinylidene fluoride membrane, blocked in 1% BSA, incubated for 1 h at room temperature in a 1:1,000 dilution of 100 µg/mL affinity-purified primary IgG, washed three times in PBS with 0.1% Tween-20, and incubated for 1 h in a 1:5,000 dilution of secondary anti-rabbit antibody coupled to alkaline phosphatase. This incubation was followed by washing to various degrees of stringency by elevation of salt, a Tris-buffered saline wash, and incubation in developer solution prepared from 100 µL of 7.5 mg/mL 5-Bromo-4-chloro-3-indolyl phosphate dissolved in 60% dimethyl formamide (DMF) in water and 100 µL of 15 mg/mL nitro blue tetrazolium dissolved in 70% DMF in water, adjusted to 50 mL with 0.1 M Tris (pH 9.5)/0.1 mM magnesium chloride.

1. Smith TG, Wu X, Franka R, Rupprecht CE (2011) Design of future rabies biologics and antiviral drugs. *Adv Virus Res* 79:345–363.
2. Cleaveland S, Fèvre EM, Kaare M, Coleman PG (2002) Estimating human rabies mortality in the United Republic of Tanzania from dog bite injuries. *Bull World Health Organ* 80(4):304–310.
3. Deshmukh DG, Damle AS, Bajaj JK, Bhakre JB, Patil NS (2011) Fatal rabies despite post-exposure prophylaxis. *Indian J Med Microbiol* 29(2):178–180.
4. Fooks AR, Rupprecht CE (2009) *Rabies* (Academic, Amsterdam), pp 605–627.
5. Novoa RR, et al. (2005) Virus factories: Associations of cell organelles for viral replication and morphogenesis. *Biol Cell* 97(2):147–172.
6. Campbell S, Rein A (1999) In vitro assembly properties of human immunodeficiency virus type 1 Gag protein lacking the p6 domain. *J Virol* 73(3):2270–2279.
7. Zlotnick A (2005) Theoretical aspects of virus capsid assembly. *J Mol Recognit* 18(6):479–490.
8. Dooher JE, Lingappa JR (2004) Conservation of a stepwise, energy-sensitive pathway involving HP68 for assembly of primate lentivirus capsids in cells. *J Virol* 78(4):1645–1656.
9. Dooher JE, Schneider BL, Reed JC, Lingappa JR (2007) Host ABCE1 is at plasma membrane HIV assembly sites and its dissociation from Gag is linked to subsequent events of virus production. *Traffic* 8(3):195–211.
10. Klein KC, et al. (2011) HIV Gag-leucine zipper chimeras form ABCE1-containing intermediates and RNase-resistant immature capsids similar to those formed by wild-type HIV-1 Gag. *J Virol* 85(14):7419–7435.
11. Lingappa JR, Dooher JE, Newman MA, Kiser PK, Klein KC (2006) Basic residues in the nucleocapsid domain of Gag are required for interaction of HIV-1 gag with ABCE1 (HP68), a cellular protein important for HIV-1 capsid assembly. *J Biol Chem* 281(7):3773–3784.
12. Lingappa JR, Hill RL, Wong ML, Hegde RS (1997) A multistep, ATP-dependent pathway for assembly of human immunodeficiency virus capsids in a cell-free system. *J Cell Biol* 136(3):567–581.
13. Reed JC, et al. (2012) HIV-1 Gag co-opts a cellular complex containing DDX6, a helicase that facilitates capsid assembly. *J Cell Biol* 198(3):439–456.
14. Lingappa JR, et al. (1994) A eukaryotic cytosolic chaperonin is associated with a high molecular weight intermediate in the assembly of hepatitis B virus capsid, a multimeric particle. *J Cell Biol* 125(1):99–111.
15. Klein KC, Dellos SR, Lingappa JR (2005) Identification of residues in the hepatitis C virus core protein that are critical for capsid assembly in a cell-free system. *J Virol* 79(11):6814–6826.
16. Klein KC, Polyak SJ, Lingappa JR (2004) Unique features of hepatitis C virus capsid formation revealed by de novo cell-free assembly. *J Virol* 78(17):9257–9269.
17. Kelly BN, et al. (2007) Structure of the antiviral assembly inhibitor CAP-1 complex with the HIV-1 CA protein. *J Mol Biol* 373(2):355–366.
18. Lemke CT, et al. (2012) Distinct effects of two HIV-1 capsid assembly inhibitor families that bind the same site within the N-terminal domain of the viral CA protein. *J Virol* 86(12):6643–6655.
19. Hopkins AL, Groom CR (2002) The druggable genome. *Nat Rev Drug Discov* 1(9):727–730.
20. Goff SP (2008) Knockdown screens to knockout HIV-1. *Cell* 135(3):417–420.
21. Alberts B (1998) The cell as a collection of protein machines: Preparing the next generation of molecular biologists. *Cell* 92(3):291–294.
22. Fulton AB (1982) How crowded is the cytoplasm? *Cell* 30(2):345–347.
23. Perica T, et al. (2012) The emergence of protein complexes: Quaternary structure, dynamics and allostery. Colworth Medal Lecture. *Biochem Soc Trans* 40(3):475–491.

24. Ozbabacan SE, Engin HB, Gursoy A, Keskin O (2011) Transient protein-protein interactions. *Protein Eng Des Sel* 24(9):635–648.

25. Khan SH, Ahmad F, Ahmad N, Flynn DC, Kumar R (2011) Protein-protein interactions: Principles, techniques, and their potential role in new drug development. *J Biomol Struct Dyn* 28(6):929–938.

26. Thompson AD, Dugan A, Gestwicki JE, Mapp AK (2012) Fine-tuning multiprotein complexes using small molecules. *ACS Chem Biol* 7(8):1311–1320.

27. Shimizu K, Toh H (2009) Interaction between intrinsically disordered proteins frequently occurs in a human protein-protein interaction network. *J Mol Biol* 392(5): 1253–1265.

28. Blobel G (2000) Protein targeting (Nobel lecture). *ChemBioChem* 1(2):86–102.

29. Jayakar HR, Jeetendra E, Whitt MA (2004) Rhabdovirus assembly and budding. *Virus Res* 106(2):117–132.

30. Majumder A, et al. (2001) Effect of osmolytes and chaperone-like action of P-protein on folding of nucleocapsid protein of Chandipura virus. *J Biol Chem* 276(33): 30948–30955.

31. Mondal A, et al. (2012) Interaction of chandipura virus N and P proteins: Identification of two mutually exclusive domains of N involved in interaction with P. *PLoS ONE* 7(4): e34623.

32. Liu P, Yang J, Wu X, Fu ZF (2004) Interactions amongst rabies virus nucleoprotein, phosphoprotein and genomic RNA in virus-infected and transfected cells. *J Gen Virol* 85(Pt 12):3725–3734.

33. Mavrakis M, et al. (2003) Isolation and characterisation of the rabies virus N degrees-P complex produced in insect cells. *Virology* 305(2):406–414.

34. Wunner WH (1991) *The Chemical Composition and Molecular Structure of Rabies Viruses* (Centers for Disease Control, Atlanta) pp 31–67.

35. Dooher JE, Lingappa JR (2004) Cell-free systems for capsid assembly of primate lentiviruses from three different lineages. *J Med Primatol* 33(5-6):272–280.

36. Lingappa JR, Newman MA, Klein KC, Dooher JE (2005) Comparing capsid assembly of primate lentiviruses and hepatitis B virus using cell-free systems. *Virology* 333(1):114–123.

37. Singh AR, Hill RL, Lingappa JR (2001) Effect of mutations in Gag on assembly of immature human immunodeficiency virus type 1 capsids in a cell-free system. *Virology* 279(1):257–270.

38. Fauman EB, Rai BK, Huang ES (2011) Structure-based druggability assessment—identifying suitable targets for small molecule therapeutics. *Curr Opin Chem Biol* 15(4):463–468.

39. Lee WC, Lee KH (2004) Applications of affinity chromatography in proteomics. *Anal Biochem* 324(1):1–10.

40. Zimmerman C, et al. (2002) Identification of a host protein essential for assembly of immature HIV-1 capsids. *Nature* 415(6867):88–92.

41. Bisbal C, Martinand C, Silhol M, Lebleu B, Salehzada T (1995) Cloning and characterization of a RNAse L inhibitor. A new component of the interferon-regulated 2-5A pathway. *J Biol Chem* 270(22):13308–13317.

42. Barthelme D, et al. (2011) Ribosome recycling depends on a mechanistic link between the FeS cluster domain and a conformational switch of the twin-ATPase ABCE1. *Proc Natl Acad Sci USA* 108(8):3228–3233.

43. Becker T, et al. (2012) Structural basis of highly conserved ribosome recycling in eukaryotes and archaea. *Nature* 482(7386):501–506.

44. Khoshnevis S, et al. (2010) The iron-sulphur protein RNase L inhibitor functions in translation termination. *EMBO Rep* 11(3):214–219.

45. Pisarev AV, et al. (2010) The role of ABCE1 in eukaryotic posttermination ribosomal recycling. *Mol Cell* 37(2):196–210.

46. Shoemaker CJ, Green R (2011) Kinetic analysis reveals the ordered coupling of translation termination and ribosome recycling in yeast. *Proc Natl Acad Sci USA* 108(51):E1392–E1398.

47. Purich DL (2001) Enzyme catalysis: A new definition accounting for noncovalent substrate- and product-like states. *Trends Biochem Sci* 26(7):417–421.

48. Albertini AA, et al. (2006) Crystal structure of the rabies virus nucleoprotein-RNA complex. *Science* 313(5785):360–363.

49. Harlow E, Lane D (1999) *Using Antibodies: A Laboratory Manual* (Cold Spring Harbor Laboratory, Cold Spring Harbor, NY).